

OSTEOARTHRITIS DIAGNOSIS VIA INNOVATIVE BIOPHYSICAL BIOMARKERS

Konstantinos Antonopoulos¹

¹ School of Engineering Sciences in Chemistry, Biotechnology and Health, KTH Royal Institute of Technology, Drottning Kristinas väg 4, 114 28 Stockholm, Sweden

* E-mail: k.antonio@outlook.com

Abstract: Osteoarthritis is the most common form of arthritis, causing pain and stiffness in affected joints. Unfortunately, to date, there is no method for accurate early diagnosis or treatment of osteoarthritis, only ways to alleviate and delay symptoms. The role of synovial fluid is crucial for the smooth functioning of the joint, as it provides the necessary mechanical properties for movement. Its main component is hyaluronic acid, which, by creating a polymeric network connected to proteins, imparts the appropriate rheological characteristics. This dissertation develops a systematic and standardized approach to data processing with the ultimate goal of evaluating biomarkers for early diagnosis of the disease. By using biomarkers, different populations are compared, the influence of specific factors is studied, and a machine learning algorithm is trained to optimize diagnostic capability. Through this specific preclinical study, the candidate biomarkers appear to possess significant diagnostic capability and can be clinically used to improve the quality of life for patients.

1 Introduction

Osteoarthritis (OA), also known as degenerative joint disease or degenerative arthritis, is one of the most common forms of arthritis and one of the leading causes of disability, chronic pain, and dysfunction for the elderly people, while the economic burden of this progressive multifactorial joint disease on patients and society is also significant [1–5]. Specific factors such as age, gender, obesity, injuries, repetitive stress on a particular joint due to occupations, genetics, muscle weakness, malalignment, bone deformities, metabolic diseases, endocrine disorders, and previous cases of rheumatic diseases constitute crucial OA risk factors [6,7]. Although any joint can be affected, it is worth noting that the knee, hands, hip, and spine are the ones getting influenced more frequently [4].

Pathological joints are characterized by alterations of the whole joint structure including progressive degradation of the articular cartilage, menisci, and ligaments, thickening of the subchondral bone, inflammation of the synovium, formation of osteophytes and hypertrophy of the joint capsule [3], [8,9]. Since there is no cure that can prevent, cease, or control the progression of OA, a great focus has been given to the prevention, early diagnosis, and treatment in the early stages of the disease aiming to improve patients' quality of life [4,5].

The role of synovial fluid (SF) is paramount when it comes to a healthy joint, since it is not only responsible for lubricating the joint, but also for transporting nutrients and oxygen to the cartilage, load bearing and shock absorption [10–12]. It can be characterized as a high molecular mass complex of hyaluronic acid (HA) chemically bound to the proteins of the blood, which makes the SF a highly viscous and viscoelastic fluid offering the necessary properties to the joint [11]. Nevertheless, in case of OA, the SF is significantly of much lower molecular weight and concentration of HA and therefore, the composition of it is altered leading to deterioration of its rheological properties and consequently, effectiveness in the joint [12–14].

In an endeavor to explain how SF could be used as a tool for the early diagnosis of OA, here we present comparative measurements of the rheological behavior of SF in human samples. With the intentions to discriminate the differences between SF samples from both cases of healthy and OA joints, the viscoelastic properties and non-Newtonian behavior of SF are studied in detail and a statistical analysis is performed.

2 Materials & Methods

2.1 Collection of Synovial Fluid Samples from Healthy & Pathological Human Joints

The sampling of the human synovial fluid was carried out by orthopedic surgeons at the 1st Orthopedic University Clinic AUTH of the Thessaloniki General Hospital "G. Papanikolaou". 61 volunteers, 23 men and 38 women, aged 21 to 93, participated. The research protocol of the study that was followed is in accordance with the Local Ethics Committee and the World Medical Association Declaration of Helsinki "Ethical Principles for Medical Research Involving Human Subjects", amended in October 2013. All patients were informed about the research and the procedure and gave their consent to participate in the study. Sampling was performed using a 21 Gauge needle under aseptic conditions and under anesthesia in the operating room. The volume of SF was at least 0.5ml. The analysts received the samples blindly, without clinical or demographic information, while the diagnosis had already been made by the doctors with clinical and imaging methods. The SF samples were immediately stored in the refrigerator at 4°C until they were measured and analyzed as soon as possible, within 48 hours.

2.2 Rheological Studies of Human Knee Synovial Fluid Samples

Rheological measurements were carried out on AR-G2 rheometer (TA Instruments), using a flat geometry (40mm diameter), made of stainless steel, at 25 °C and 37 °C (human's normal temperature) with the lower parallel Peltier plate having a temperature accuracy of ± 0.1 °C. Depending on the sufficiency of the samples, priority was given to measurements at 25 °C. A plastic cover was applied around the plates in order to slow down sample evaporation during the experiment. The volume of each aliquot ranged from 0.30 to 0.40 mL with a gap between the two plates from 240 to 320 microns. In order to verify the accuracy of the rheometer, the S60 Viscosity Standard Oil by Cannon Instrument Company was used to measure the systematic errors of the device, which were found to be around 5-9% at 25 °C for both oscillatory and steady state measurements. Two types of measurements were performed in the rheometer, dynamic oscillatory, and steady state flow ones. Oscillatory measurements included Time Sweep test which measures the elastic G and viscous G' as a function of time, Frequency Sweep test which measures the

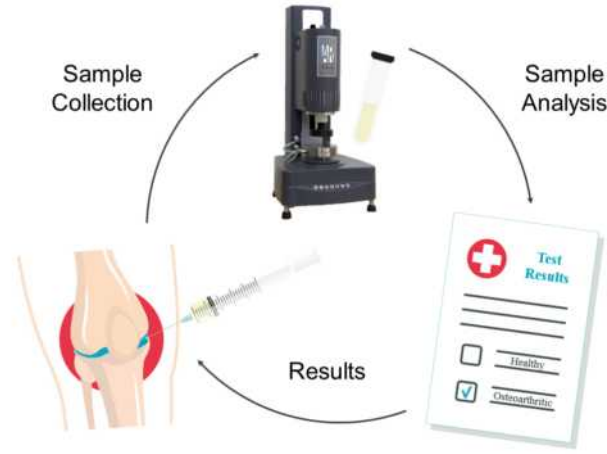


Fig. 1: Schematic representation of the workflow used in this study. Synovial fluid from 18 OA patients and 5 healthy individuals was analyzed using an AR-G2 rheometer. Statistical analysis and classification models was used to compare OA and healthy individuals and identify OA-associated biophysical biomarkers. The models for cancer classification were generated using machine learning techniques utilizing artificial samples that were created via Monte Carlo simulation (60% of the data in training set).

alteration of the same variables and the dynamic viscosity as a function of oscillation frequency and Strain Sweep test which measures the alteration of G' and G'' as a function of the range of oscillation of the strain stress at a specified value of the oscillation frequency of the geometry. The strain applied to the first two tests was 3%, which is in the Linear Viscoelastic Region (LVR) as known from the literature and observed from the Strain Sweep. The angular frequency of oscillation for Time and Strain Sweep measurements was 0.5 Hz (3.142 rad/s). Steady state flow measurements included Flow Step which measures the viscosity of the sample during the rotation of the geometry at increasing shear rates. The shear rate range is 0.1 - 2000 (s⁻¹).

2.3 Sample Preprocessing Pipeline Standardization

The sample preprocessing pipeline was standardized to ensure data quality prior to entry into the database. Quality control assessment involved the implementation of specific filters targeting outlier values and deviations.

Values exceeding predefined thresholds for the Cross Over Point (rad/s), as well as values outside acceptable ranges for other model parameters including Zero-rate Viscosity (Pa.s), Infinite-rate Viscosity (Pa.s), Consistency (s), Rate Index (-), and Standard Error (-), were assigned NaN values. Experiments deviating more than 20% from other experiments of the same sample were also filtered and assigned NaN values.

2.4 Statistical Analysis

Statistical analysis involved two-sided independent t-tests between distinct populations utilizing the scipy.stats Python library. This method was employed to assess differences between experimental groups with statistical significance.

2.5 Data Visualization

Visualization of the data was conducted using the matplotlib and seaborn Python libraries. These tools facilitated the graphical representation of trends and patterns within the dataset.

2.6 Machine Learning Model Training

Artificial data generation was undertaken to augment the dataset for machine learning model training. These artificial samples were generated based on the distributions observed in real samples via Monte Carlo simulation.

Machine learning classification models were trained using 60% of the augmented dataset as a training set, with the remaining 40% reserved for testing. The trained models were subsequently evaluated on real data to assess their performance. The scikitlearn library was utilized for model development and evaluation.

3 Results

Figure 1 shows an overview of our workflow used to identify OA-associated biophysical biomarkers based on both statistical analysis and classification models.

3.1 Determination of Linear Viscoelastic Region

When viscoelastic properties of fluids are measured, it is crucial to identify the Linear Viscoelastic Region (LVR), characterized by stress increasing proportionally to deformation. Within this region, material structure remains intact, enabling accurate measurement of microstructural properties. Figure 2 depicts three representative Strain Sweep experiments aimed at delineating the point at which the modulus of elasticity, G' , exhibits dependency on stress or deformation, delineating the LVR [15]. Two experiments were conducted at 25 °C, one at 0.5 Hz, and the other at 2.5 Hz, while the third was conducted at 37 °C and 0.5 Hz. Notably, all three samples exhibit LVR behavior up to 10% strain. Below 2% strain, noise interferes significantly, compromising measurement accuracy. Consequently, studying rheological properties of the sample within the 2-10% strain range is recommended. Furthermore, frequency increase correlates with rapid experimental value escalation, while temperature rise leads to mild value reduction.

3.2 Rheological Characterization of Osteoarthritic Human Knee Synovial Fluid (SF)

Figure 3 presents comprehensive rheological analyses including Time Sweep (A), Frequency Sweep (B), Flow Step (C), and Cox-Merz rule (D) measurements for an osteoarthritic human knee SF sample.

The evolution of G' and G'' over time at 25°C is depicted for the osteoarthritic SF sample. Both G' and G'' exhibit stability over time, indicating independence from temporal factors. To ensure data reliability, only values recorded after the initial minute, allowing for thermal equilibrium, were considered.

At lower frequencies of oscillation, the viscous behavior (G'') dominates over the elastic behavior (G') in the osteoarthritic SF sample, whereas at higher frequencies, the reverse holds true. The

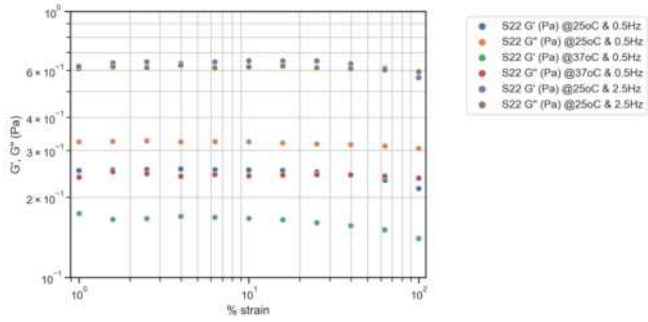


Fig. 2: Strain Sweep at 25 oC and 0.5 Hz (G' - blue, G'' - orange), at 37 oC and 0.5 Hz (G' - green, G'' - red) and at 25 oC and 2.5 Hz (G' - purple, G'' - brown).

crossover point at 1.4 rad/s signifies the angular frequency at which G' equals G'' , attributed to transient entanglements of hyaluronic acid chains [16–18].

The viscosity alteration with increasing shear rate of the osteoarthritic SF sample is illustrated. Shear thinning behavior, observed with a Newtonian Plateau at low to medium shear rates, aligns with prior research findings and can be effectively modeled via the Cross model [18–20].

The Cox-Merz rule comparison for the osteoarthritic SF sample demonstrates strong agreement between dynamic oscillatory and steady-state experiments. Minor discrepancies observed at high angular frequencies may be attributed to inertia effects.

3.3 Comparison between Healthy and Osteoarthritic Human Knee Synovial Fluid Samples

Figure 4 presents a comparative analysis of G' and G'' values between healthy and osteoarthritic (OA) samples across three different frequencies. Through frequency sweep experiments on various samples, both the mean and standard deviations of rheological parameters were computed. The first two pairs of bars represent G'

and G'' values at 0.68 rad/s (0.1 Hz), the third and fourth pairs at 3.14 rad/s (0.5 Hz), and the final two pairs at 14.58 rad/s (2.3 Hz).

Overall, healthy samples exhibit substantially higher G' and G'' values compared to OA samples across all frequencies. While G' tends to increase from low to high frequencies, the G'' values remain relatively constant after 3.14 rad/s. This observation suggests a transition to more elastic behavior at higher frequencies, where the elastic character of the material overrides its viscous nature.

Additional biomarker analyses are presented in Figures 5 and 6. Figure 5 compares the values of n and $\ln|n|$ between healthy and OA samples, revealing higher values of both biomarkers in healthy samples. Notably, none of the samples in the healthy group passed quality control for the n biomarker. In Figure 6, the difference between healthy and OA samples for $\tan(\delta)$ is depicted at three different frequencies (0.68, 3.14, and 14.58 Hz). Once again, healthy samples consistently exhibit lower values compared to OA samples across all frequencies.

In Table 1 and 2 the t-test results and the binary classification metrics respectively, are summarized for all biomarkers together. In Figure 7, the ROC analysis demonstrates the performance of the best single-feature classification model. The selected feature was G' at 3.142 rad/s. The resulting AUC, approaching 1, indicates nearly perfect classification accuracy.

4 Discussion

Understanding the rheological behavior of synovial fluid, particularly in the context of osteoarthritis, holds significant clinical relevance. Our study delves into the dynamic nature of synovial fluid, shedding light on its mechanical properties and potential implications for disease diagnosis and management.

Analysis of rheological experiments provides valuable insights into the viscoelastic behavior of synovial fluid. We observe a transition from predominantly viscous behavior at lower frequencies to more elastic behavior at higher frequencies. This transition underscores the complexity of synovial fluid dynamics, reflecting its ability to withstand varying levels of stress and deformation.

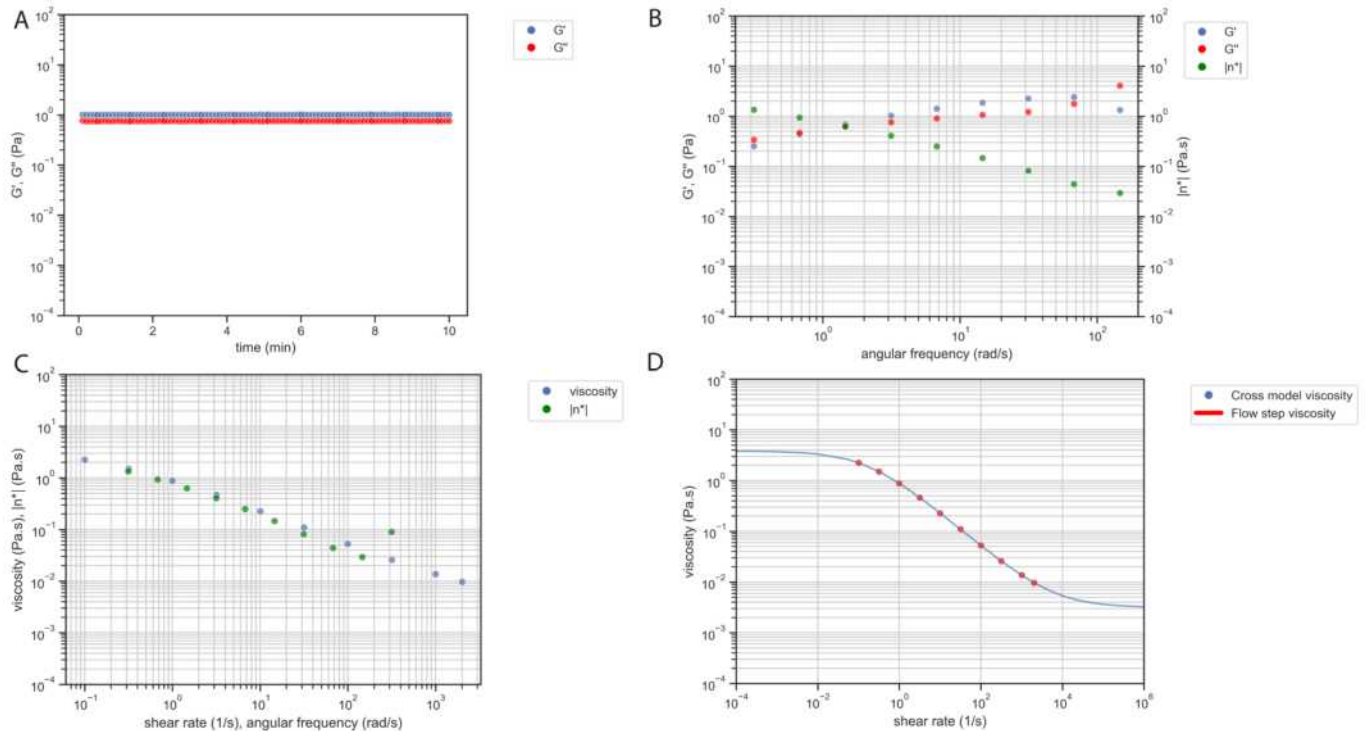


Fig. 3: Time Sweep (A), Frequency Sweep (B), Flow Step with Cross model (C) and the application of Cox-Merz rule (D) for healthy and OA HSF samples.

Moreover, our findings highlight distinct rheological profiles between healthy and osteoarthritic samples. Healthy samples consistently exhibit superior mechanical properties across different frequencies, suggesting a potential diagnostic utility for rheological parameters in distinguishing between healthy and diseased synovial fluid samples. Additionally, biomarker analysis further supports these observations, emphasizing the clinical relevance of rheological assessments in osteoarthritis diagnosis and management.

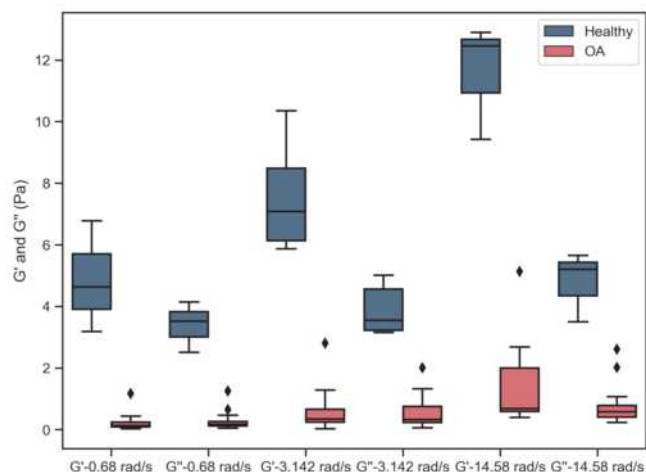


Fig. 4: Comparison of G' and G'' between healthy and OA human knee SF samples at 25 °C and at three different frequencies. G' and G'' at 0.68, 3.42, and 14.58 rad/s respectively.

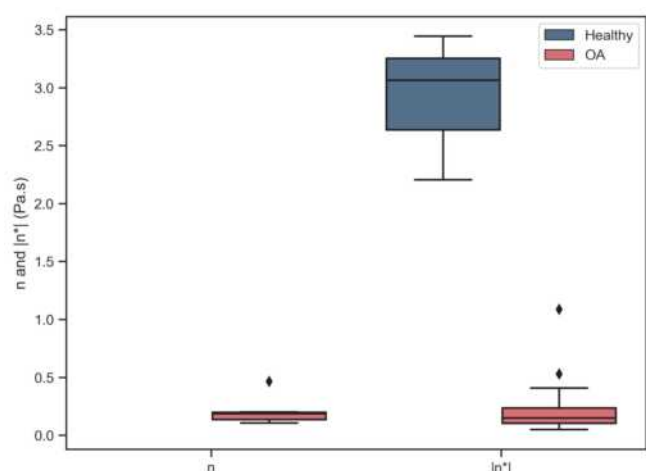


Fig. 5: Comparison of n and $|n^*|$ between healthy and OA human knee SF samples at 25 °C.

These insights contribute to our understanding of the pathophysiology of osteoarthritis and hold promise for future diagnostic and therapeutic advancements. By elucidating the rheological characteristics of synovial fluid, our study provides a foundation for further research aimed at improving clinical outcomes for patients with osteoarthritis.

5 References

1 S. Tarafder and C. H. Lee, Synovial Joint: In Situ Regeneration of Osteochondral and Fibrocartilaginous Tissues by Homing of Endogenous Cells. Elsevier Inc., 2016. doi: 10.1016/B978-0-12-802225-2.00014-3.

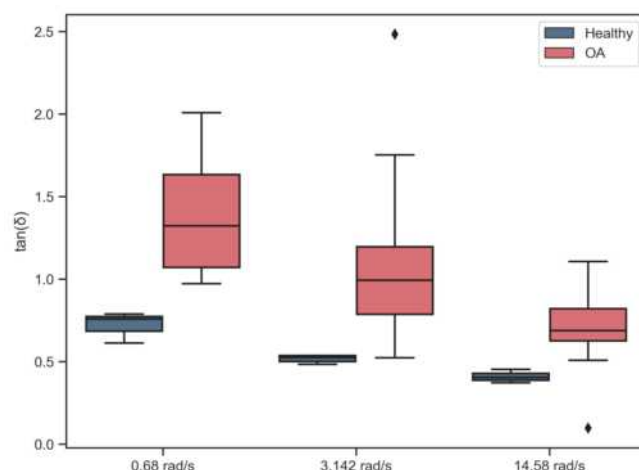


Fig. 6: Comparison of $\tan(\delta)$ between healthy and OA human knee SF samples at 25 °C and at three different frequencies. $\tan(\delta)$ at 0.68, 3.42, and 14.58 rad/s respectively.

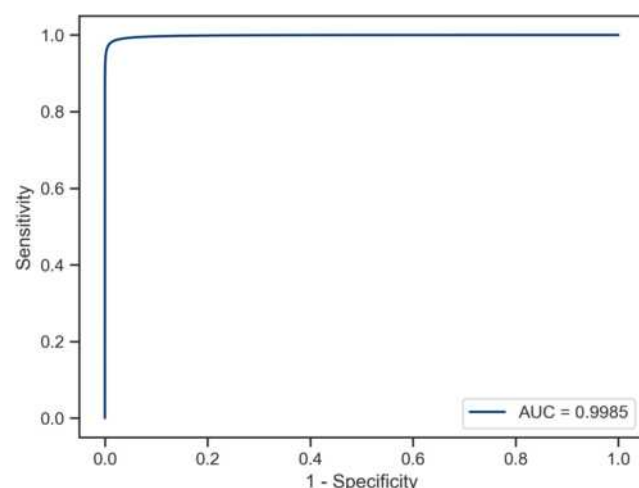


Fig. 7: ROC Analysis: Evaluating Classification Model Performance with G' at 3.142 rad/s as a Feature

- 2 A. D. Pearle, R. F. Warren, and S. A. Rodeo, "Basic science of articular cartilage and osteoarthritis," Clin Sports Med, vol. 24, no. 1, pp. 1–12, 2005, doi: 10.1016/j.csm.2004.08.007.
- 3 R. F. Loeser, S. R. Goldring, C. R. Scanzello, and M. B. Goldring, "Osteoarthritis: A disease of the joint as an organ," Arthritis Rheum, vol. 64, no. 6, pp. 1697–1707, 2012, doi: 10.1002/art.34453.
- 4 M. Kloppenburg and F. Berenbaum, "Osteoarthritis in review 2019: epidemiology and therapy," Osteoarthritis Cartilage, vol. 28, no. 3, pp. 242–248, 2020, doi: 10.1016/j.joca.2020.01.002.
- 5 A. Cui, H. Li, D. Wang, J. Zhong, Y. Chen, and H. Lu, "Global, regional prevalence, incidence and risk factors of knee osteoarthritis in population-based studies," EclinicalMedicine, vol. 29–30, p. 100587, 2020, doi: 10.1016/j.eclinm.2020.100587.
- 6 A. Mobasheri and M. Batt, "An update on the pathophysiology of osteoarthritis," Ann Phys Rehabil Med, vol. 59, no. 5–6, pp. 333–339, 2016, doi: 10.1016/j.rehab.2016.07.004.
- 7 X. Wang, D. J. Hunter, X. Jin, and C. Ding, "The importance of synovial inflammation in osteoarthritis: current evidence from imaging assessments and clinical trials," Osteoarthritis Cartilage, vol. 26, no. 2, pp. 165–174, 2018, doi: 10.1016/j.joca.2017.11.015.
- 8 J. W. J. Bijlsma, F. Berenbaum, and F. P. J. G. Lafeber, "Osteoarthritis: An update with relevance for clinical practice," The Lancet, vol. 377, no. 9783, pp. 2115–2126, 2011. doi: 10.1016/S0140-6736(11)60243-2.

- 9 M. K. Kosinska et al., "Comparative lipidomic analysis of synovial fluid in human and canine osteoarthritis," *Osteoarthritis Cartilage*, vol. 24, no. 8, pp. 1470–1478, Aug. 2016, doi: 10.1016/j.joca.2016.03.017.
- 10 F. Bronner and M. C. Farach-Carson, *Bone and osteoarthritis*. - (Topics in Bone Biology; v. 4), vol. 4. Springer-Verlag London Limited 2007, 2007.
- 11 J. Schurz and V. Ribitsch, "Rheology of Synovial Fluid," Copyright (c) 1987 Pergamon Journals Ltd. All rights reserved, no. c, pp. 385–399, 1987.
- 12 H. Fam, J. T. Bryant, and M. Kontopoulou, "Rheological properties of synovial fluids," IOS Press, 2007.
- 13 C. Backus, S. P. Carrington, L. R. Fisher, J. A. Odell, and D. A. Rodrigues, *the Roles of Extensional and Shear Flows of Synovial Fluid and Replacement Systems in Joint Protection*. Woodhead Publishing Ltd, 2002. doi: 10.1533/9781845693121.209.
- 14 P. Bhuanantanondh, "RHEOLOGY OF SYNOVIAL FLUID WITH AND WITHOUT VISCOSUPPLEMENTS IN PATIENTS WITH OSTEOARTHRITIS: A PILOT STUDY," 2009.
- 15 Malvern Instruments. (2016). *A Basic Introduction to Rheology*. [16] Milas, M.; Rinaudo, M. Characterization and properties of hyaluronic acid (hyaluronan). In *Polysaccharides*; CRC Press: Boca Raton, FL, USA, 2004.
- 17 Milas, M.; Rinaudo, M.; Roure, I.; Al-Assaf, S.; Phillips, G.O.; Williams, P.A. Comparative rheological behavior of hyaluronan from bacterial and animal sources with cross-linked hyaluronan (hylan) in aqueous solution. *Biopolymers* 2001, 59, 191–204.
- 18 Yu, F.; Zhang, F.; Luan, T.; Zhang, Z.; Zhang, H. Rheological studies of hyaluronan solutions based on the scaling law and constitutive models. *Polymer* 2014, 55, 295–301.
- 19 Krause, W.E.; Bellomo, E.G.; Colby, R.H. Rheology of sodium hyaluronate under physiological conditions. *Biomacromolecules* 2001, 2, 65–69.
- 20 Braithwaite, G.J.; Daley, M.J.; Toledo-Velasquez, D. Rheological and molecular weight comparisons of approved hyaluronic acid products—Preliminary standards for establishing class iii medical device equivalence. *J. Biomater. Sci. Polym. Ed.* 2016, 27, 235–246.

Table 1 T-test results.

<i>Biomarker</i>	<i>t – statistic</i>	<i>p – value</i>
G' at 0.68 rad/s (Pa)	10.49	1.03e-07
G'' at 0.68 rad/s (Pa)	8.66	9.35e-07
G' at 3.142 rad/s (Pa)	10.81	8.36e-10
G'' at 3.142 rad/s (Pa)	8.35	5.92e-08
G' at 14.58 rad/s (Pa)	6.26	2.91e-05
G'' at 14.58 rad/s (Pa)	5.79	6.29e-05
Viscosity [η^*] at 3.142 rad/s	5.33	1.36E-03
tan(δ) at 0.68 rad/s	-3.64	3.00e-03
tan(δ) at 3.142 rad/s	-3.26	3.88e-03
tan(δ) at 14.58 rad/s	-1.79	9.63e-02

Table 2 Biomarker evaluation - Binary classification metrics.

<i>Biomarker</i>	<i>Sensitivity</i>	<i>Specificity</i>	<i>Accuracy</i>	<i>Youden's Index</i>
G' at 0.68 rad/s	1.0	1.0	1.0	1.0
G'' at 0.68 rad/s	1.0	1.0	1.0	1.0
G' at 3.142 rad/s	1.0	1.0	1.0	1.0
G'' at 3.142 rad/s	1.0	1.0	1.0	1.0
G' at 14.58 rad/s	1.0	1.0	1.0	1.0
G'' at 14.58 rad/s	1.0	1.0	1.0	1.0
Viscosity [η^*] at 3.142 rad/s	1.0	1.0	1.0	1.0
tan(δ) at 0.68 rad/s	1.0	1.0	1.0	1.0
tan(δ) at 3.142 rad/s	0.94	1.0	0.95	0.94
tan(δ) at 14.58 rad/s	0.92	1.0	0.93	0.92